

AD-A222 402

OFFICE OF NAVAL RESEARCH

Contract: N00014-85-K-0222

Work Unit: 4327-555

Scientific Officer: Dr. Richard S. Miller

Technical Report No. 25

MODEL STUDIES OF THE EFFECT OF SURFACE ROUGHNESS
AND MECHANICAL INTERLOCKING ON ADHESION

by

A. N. Gent and C.-W. Lin

Institute of Polymer Engineering
The University of Akron
Akron, Ohio 44325

May, 1990

Reproduction in whole or in part is permitted for

any purpose of the United States Government

Approved for public release; distribution unrestricted

DTIC
ELECTE
MAY 25 1990
S E D

REPORT DOCUMENTATION PAGE		READ INSTRUCTIONS BEFORE COMPLETING FORM
1. REPORT NUMBER Technical Report No. 25	2. GOVT ACCESSION NO.	3. RECIPIENT'S CATALOG NUMBER
4. TITLE (and Subtitle) Model Studies of the Effect of Surface Roughness and Mechanical Interlocking on Adhesion		5. TYPE OF REPORT & PERIOD COVERED Technical Report
		6. PERFORMING ORG. REPORT NUMBER
7. AUTHOR(s) A. N. Gent and C.-W. Lin		8. CONTRACT OR GRANT NUMBER(s) N00014-85-K-0222
9. PERFORMING ORGANIZATION NAME AND ADDRESS Institute of Polymer Engineering The University of Akron Akron, Ohio 44325-0301		10. PROGRAM ELEMENT, PROJECT, TASK AREA & WORK UNIT NUMBERS 4327-555
11. CONTROLLING OFFICE NAME AND ADDRESS Office of Naval Research Power Program Arlington, VA 22217-5000		12. REPORT DATE May 1990
		13. NUMBER OF PAGES 34
14. MONITORING AGENCY NAME & ADDRESS (if different from Controlling Office)		15. SECURITY CLASS. (of this report) Unclassified
		15a. DECLASSIFICATION/DOWNGRADING SCHEDULE
16. DISTRIBUTION STATEMENT (of this Report) According to attached distribution list. Approved for public release; distribution unrestricted.		
17. DISTRIBUTION STATEMENT (of the abstract entered in Block 20, if different from Report)		
18. SUPPLEMENTARY NOTES Submitted to: Journal of Adhesion Gent		
19. KEY WORDS (Continue on reverse side if necessary and identify by block number) Adhesion, Cloth, Elastomers, Fracture, Interlocking, Rubber, Strength, Surface Roughness (S)		
20. ABSTRACT (Continue on reverse side if necessary and identify by block number) The apparent strength of adhesion has been measured for a soft elastic layer adhering to model porous substrates, consisting of rigid plates containing regular arrays of cylindrical holes. Two contributions to the apparent strength have been identified and compared with the predictions of a simple theoretical treatment. The first is adhesion to the surface itself. Because "rough" surfaces have greater area for bonding, the (over)		

strength of adhesion was increased by as much as twenty-fold. The second arises from the work of breaking deeply embedded or entangled strands in order to detach the overlayer. Contributions from this mechanism were as much as several hundred times the (low) intrinsic strength of adhesion. Satisfactory agreement was obtained with theory in both cases. Measurements were also made using cloth substrates, when the adhering layer penetrated the cloth completely. The work of detaching and breaking permeating strands was again much larger than the intrinsic strength of adhesion, in reasonable agreement with theoretical predictions.

Accession For	
NTIS GRA&I	<input checked="" type="checkbox"/>
DTIC TAB	<input type="checkbox"/>
Unannounced	<input type="checkbox"/>
Justification	
By	
Distribution/	
Availability Codes	
Dist	Avail and/or Special
A-1	



To appear in: J. Adhesion

Model Studies of the Effect of Surface Roughness and Mechanical
Interlocking on Adhesion

A.N. Gent and C.-W. Lin

College of Polymer Science and Polymer Engineering

The University of Akron, Akron, Ohio, 44325-0301

ABSTRACT

The apparent strength of adhesion has been measured for a soft elastic layer adhering to model porous substrates, consisting of rigid plates containing regular arrays of cylindrical holes. Two contributions to the apparent strength have been identified and compared with the predictions of a simple theoretical treatment. The first is adhesion to the surface itself. Because "rough" surfaces have greater area for bonding, the strength of adhesion was increased by as much as twenty-fold. The second arises from the work of breaking deeply embedded or entangled strands in order to detach the overlayer. Contributions from this mechanism were as much as several hundred times the (low) intrinsic strength of adhesion. Satisfactory agreement was obtained with theory in both cases. Measurements were also made using cloth substrates, when the adhering layer penetrated the cloth completely. The work of detaching and breaking permeating strands was again much larger than the intrinsic strength of adhesion, in reasonable agreement with theoretical predictions.

Keywords

Cloth, Adhesion to
Elastomers, Adhesion of
Mechanical Interlocking

Porous Substrates
Rubber, Adhesion of
Surface Roughness

1. Introduction

Although the importance of surface roughness in adhesion has often been emphasized, there have been few quantitative studies of the effect¹⁻⁴. A rough surface presents a greater real area for bonding than a smooth surface, but this seems unlikely to increase the apparent work of detachment per unit of projected area by more than about 100 per cent. For example, a surface consisting entirely of protruding ridges, with a peak angle of 60° , would only have twice as much surface for bonding as a flat surface of the same projected area.

On the other hand, a deeply-pitted surface may have several times its apparent (planar) area. In addition, the mechanics of pulling out strands of an elastic material from deep pits leads to a substantial increase in the work of detachment. In the limit, if the adhering material thoroughly permeates a porous substrate, it may not be possible to pull out embedded strands without fracturing them. Adhesives that penetrate cloth fall into this category.

We consider here two simple models of "rough" substrates: a flat surface containing deep cylindrical holes which the adhesive fills, and a perforated plate completely filled by adhesive and with a layer of adhesive on each side. In the first case the strands of adhesive are assumed to pull out of the holes. In the second, the strands are connected at each end to a continuous overlayer of adhesive. They are thus forced to break when one layer is pulled off. In both cases the adhesive is treated as an elastic solid.

Theoretical relations are derived for the additional work required to remove an overlying layer of the adhesive, compared to that for detaching it from a flat surface of the same substrate. They are presented below.

Experiments have been carried out with layers of rubber molded in contact with aluminum surfaces, both flat and pitted with cylindrical holes of various diameters and depths. Also, measurements have been made for rubber layers molded in contact with, and completely permeating, open-mesh woven-wire cloth. The results are reported in subsequent sections, and compared with theoretical predictions.

The present problem is similar in some ways to that considered by Wake⁵. He studied the increase in adhesion caused by protruding fibers of cloth that become embedded in an elastomeric adhesive layer applied to the cloth. If the fibers are relatively extensible in comparison with rubber, then the present theoretical treatment would apply in that case also. But fibers are generally much stiffer than elastomers. The mechanics of pull-out of rigid rods embedded in an elastic half-space is more complex than for the pull-out of elastic rods from a rigid half-space because the stress distribution is not known, at least as far as the present authors are aware. Quantitative analysis of the "Wake" effect must therefore be postponed until the corresponding elastic problem has been solved.

A frictional contribution to the work of detachment may be significant for some porous substrates, when the permeating strands are long and thin, but it is ignored here in comparison with the work of separation and fracture. Further experiments would be highly

desirable to evaluate the frictional contribution.

2. Theoretical predictions

(a) Pull-out of embedded elastic strands

The work w_1 required to pull a single strand out of a cylindrical hole is obtained from the product of the pull-out force F and the amount that the strand is stretched as it is pulled out, given by the product of its extension e under the force F and its length l . Thus,

$$w_1 = Fel. \quad (1)$$

The tensile strain e in the strand is given by

$$e = F/\pi a^2 E \quad (2)$$

for a cylindrical strand of radius a made of a linearly-elastic material of Young's (tensile) modulus E .

By equating the change in energy of the system as the length of the detached portion increases to the energy expended in detaching, the pull-out force is obtained as⁶

$$F^2 = 4\pi^2 a^3 E G_a \quad (3)$$

where G_a is the characteristic work of detachment of the adhering material from the substrate, per unit of bonded area - a measure of the strength of adhesion.

From Equations 1, 2 and 3,

$$w_1 = 4\pi a l G_a. \quad (4)$$

Thus, the additional work required to pull a strand out is exactly twice that expected from the additional bonded area. (The rest is expended in stretching the strand as it detaches.)

If there are n holes per unit area of the substrate, then the extra work $w = nw_1$. But the area bonded in the normal way is reduced from unity to $1 - n\pi a^2$. The net effect is to increase the work of detachment per unit of apparent area of substrate from G_a to G'_a , where

$$G'_a/G_a = 1 - n\pi a^2 + 4\pi n a l. \quad (5)$$

Putting φ for the total area of holes per unit area of substrate, where $\varphi = n\pi a^2$,

$$G'_a/G_a = 1 + [4(l/a) - 1]\varphi. \quad (6)$$

Equation 6 predicts that the work of detachment is increased only if the depth l of the holes is greater than one-fourth of their radius. But adhesion to the substrate material at the base of the holes has been neglected so far. If we make the simple assumption that adhesion at these sites is exactly equivalent to adhesion at the surface, then Equation 6 becomes

$$G'_a/G_a = 1 + 4\varphi(l/a). \quad (7)$$

For deep holes, with $l/a \gg 1$, the work of detachment is predicted to be much greater than the value G_a for a flat surface. Indeed, it can easily exceed the work of fracture of the overlying layer when G_a is large and the holes are relatively deep. Thus, we reach the surprising conclusion that the work required to detach an adhering layer from a rough surface can exceed the work of cohesive rupture of the layer, because of the large amount of extra work expended in stretching and detaching long protruding threads, without any of the threads actually breaking.

It should be noted that work dissipated in the overlayer is neglected in these theoretical calculations. Only work expended in stretching the strands is considered. Thus, the real work of detachment may well be considerably larger.

(b) Breaking of strands

When the pores in the substrate interconnect, there is no way of pulling out a strand without breaking it. This situation arises when an adhesive permeates cloth, for example. In an attempt to take into account the work of strand rupture, we replace the complex network of permeating strands by an array of cylindrical threads, perpendicular to the plane of the substrate surface, and consider the work required to break them.

Taking the work U_b of rupture of the material per unit volume as a measure of its strength, the work w_2 required to break a single strand

is given by

$$w_2 = \pi a^2 \ell U_b. \quad (8)$$

For an array of n strands per unit area the corresponding contribution to the work of detachment is

$$\Delta G_a = n\pi a^2 \ell U_b = \varphi \ell U_b. \quad (9)$$

Equation 9 is similar to that derived by Gent and Thomas to account for the tear strength of foamed materials, considered as a network of connected strands⁷.

Thus, if strands must be broken as well as pulled loose from the holes in which they are embedded, the apparent work of detachment G'_a becomes

$$G'_a = G_a [1 + 4(\ell/a)\varphi] + \ell U_b \varphi \quad (10)$$

where ℓ denotes the length of a strand between the point at which it is held fast and the upper layer, i.e., the length that is stretched to break. Note that the first term on the right-hand side of Equation 9 depends only upon the "aspect ratio" ℓ/a of the strands, whereas the second term depends directly on their length ℓ . For shallow pores, therefore, the second term will be small but for deep pores it will become dominant.

Some experimental measurements of the work of detachment of elastic layers adhering to models of porous substrates are described in the

following sections of this paper and compared to the theoretical predictions developed above.

3. Experimental details

Perforated aluminum plates of thickness 1.6 to 9.2 mm were prepared with regular arrays of cylindrical holes, radius 0.77 to 1.3 mm, drilled through them. The holes were placed at various spacings so that the fractional area ϕ of plate surface occupied by holes varied from about 0.1 to 0.5. Care was taken to remove rough edges from the holes by countersinking them slightly and polishing the edges.

The plates were treated by the FPL (Forest Product Laboratories) process (4) to give a standard, reproducible, oxide surface. An unvulcanized rubber compound was then pressed into contact with the plates so that the rubber formed a continuous layer on top, about 1.5 mm thick, and filled the holes completely. The rubber compound was then vulcanized in this position, by heating the assembly in a hot press for periods of 30-60 min at temperatures of 141-150°C. In some instances, a layer of plastic material was placed underneath the aluminum plate to seal the lower end of the holes. Rubber in the holes then formed cylindrical threads attached to the rubber overlayer and penetrating to the bottom of the holes, but not further. These specimens were used for "pull-out" experiments. In other cases, the rubber threads passed right through the holes to join an identical rubber layer placed on the other side of the plate. These specimens were used for "tearing" experiments, because the upper rubber layer could not be removed without breaking the interconnecting threads.

Other experiments were carried out using stainless steel woven-wire cloth, having a loose square weave. Rubber layers were placed on either side of a piece of wire cloth so that the rubber completely penetrated it during molding and vulcanization. Again, therefore, strands of rubber were necessarily broken in detaching one of the rubber layers, either at 90° or in T-peeling, Figure 1.

Wire diameters d ranged from 0.2 to 0.6 mm. Rubber strand lengths l were taken as twice the wire diameter, and this was approximately the same as the overall thickness of the cloth. Viewed from on top, gaps between the wires appeared to be square holes, with lengths of side ranging from 0.13 to 1.0 mm. The cross-sectional area of a rubber strand was taken to be the same as the area of this projected hole, although the strands actually had complex cross-sections, somewhat larger than the apparent hole size. Dimensions of the wires and holes are given in Table 1, together with values of ϕ calculated from them.

Two different elastomers were used as adhering layers, giving soft rubbery materials of similar elastic modulus but of widely-different strength. They were: natural rubber (NR) and a styrene-butadiene copolymer (SBR). The mix recipes and vulcanization conditions are given in the Appendix. The tensile breaking energy U_b was determined for each material from the area under the tensile stress-strain relation up to the breaking point. Values were obtained of 19 MJ/m^3 for the natural rubber vulcanizate and 3.0 MJ/m^3 for the SBR vulcanizate. Measurements were made of the peeling energy for a layer of each material, 20 mm wide, vulcanized in contact with a flat

aluminum plate treated by the FPL process, for comparison with the energy expended in peeling a similar layer away from a perforated aluminum plate, when rubber threads were pulled out simultaneously. Values were obtained of $35 \pm 2 \text{ J/m}^2$ for the NR vulcanizate and $34 \pm 3 \text{ J/m}^2$ for the SBR vulcanizate.

In all cases the rubber overlayer was about 1.25 mm thick. A thin cotton cloth was embedded in it before vulcanization so that it could be peeled away from the aluminum plate without being stretched appreciably. Peel experiments were carried out at a rate of 5 mm/min and at a peel angle of 90° . Fracture energies for tearing away the rubber overlayer, when the rubber threads passed right through a perforated aluminum plate or a woven wire cloth, to join a similar rubber layer on the other side, were determined by peeling away at 90° and in a symmetrical way (T-peeling), as shown schematically in Figure 1. All experiments were carried out at room temperature, about 23°C .

Peel and fracture energies were calculated from the following relations:

$$G'_a = F/w \text{ for } 90^\circ \text{ peeling and} \quad (11)$$

$$G'_a = 2F/w \text{ for T-peeling.} \quad (12)$$

In each experiment the peel force F was averaged over a peel distance of about 15 mm distance. Each result given below represents the average of three similar experiments.

4. Experimental results and discussion.

(a) Pull-out of strands

Apparent values of the work G_a' of detachment are given in Table 2 for NR molded in contact with aluminum plates having cylindrical holes in them. The depth of holes ranged from 1.6 to 9.2 mm, their radius from 0.77 to 1.3 mm, and the fractional surface area occupied by holes from 0.1 to 0.5. As a result, the work of detachment was increased from the value on a smooth surface, 35 J/m^2 , by factors ranging from 2X to 20X, as shown in Table 2 and Figure 2.

Values calculated from Equation 7, taking into account the work of stretching threads as they are detached, are included in Table 2 and are represented in Figure 2 by the full line. They are seen to be similar to the measured values in all cases, lending support to the simple theory leading to Equation 7. It is clear that the extra work of pulling out threads can greatly increase the work of detachment.

(b) Tearing of strands

In order to isolate the work of breaking threads from the work of detaching them, specimens were prepared using perforated aluminum plates sprayed with a mold release agent before rubber layers were molded in contact with them. Two rubber layers were placed on either side of a plate so that the rubber threads passed through the plate and joined them together, Figure 1. Then, when the layers were peeled apart, the threads were forced to break. When there is no direct adhesion, Equation 10 becomes

$$G'_a = 2U_b \phi. \quad (13)$$

Experiments were carried out with both the strong NR material and the weak SBR material. Results are given in Table 3 for detachment at 90° , i.e., with the upper rubber layer peeled away at 90° and the lower layer held flat against the other side of the perforated plate, Figure 1a. The results for NR, when the work of detachment reached extremely high values, up to 13 kJ/m^2 , are plotted in Figure 3 against the geometrical term 2ϕ . For SBR the results are shown in Figure 4.

Equation 13 predicts a linear relationship in this representation, with a slope of U_b . The full lines in Figures 3 and 4 are drawn with the corresponding slopes. They are seen to be in satisfactory agreement with the experimental points. Values of the work of detachment G'_a calculated from Equation 13 are included in Table 3 for comparison with the directly measured values. They are seen to be in generally good agreement over the entire experimental range.

However, results from a symmetrical test arrangement, Figure 1b, gave considerably larger values for G'_a , nearly twice as large in some instances. This anomaly is attributed to the inapplicability of Equation 12 when relatively few rubber threads are stretched at the same time. Equations 11 and 12 are based on a summation of the forces in threads stretched to various degrees on the way to break, the total work of breaking them being provided by the force F . When there are only a few threads under tension simultaneously, then the integration becomes invalid and should be replaced by a simple summation of forces.

In particular, when a few threads are stretched to break simultaneously, then the forces for 90° detachment, Figure 1a, become equal to those for symmetrical detachment, Figure 1b, and the apparent work of detachment calculated from Equation 11 becomes twice as large as that calculated from Equation 10.

(c) Peeling from open-weave wire cloth

Specimens were prepared by pressing two layers of rubber on either side of a sheet of square-woven stainless steel wire cloth so that the rubber completely permeated the cloth before it was vulcanized. The wire cloths were sprayed with a silicone mold release agent before use, to minimize both adhesion and friction of the rubber in contact with the wire and thus permit the fracture contribution to apparent adhesion to be isolated.

Experiments were carried out in both 90° peeling and T-peeling. In the former case, the wire cloth and lower rubber layer were held flat by means of two long parallel metal clamps and the upper rubber layer, only 8 mm wide in these experiments instead of 20 mm wide, was peeled away at 90° . Bending of the wire cloth was prevented in this way, even when NR samples, requiring relatively large peel forces to detach them, were used.

Results are shown in Figures 5 and 6, for samples of NR and SBR, respectively. They are compared with the predictions of Equation 13, represented by the full lines in Figures 5 and 6. Reasonably satisfactory agreement is seen to hold between the theoretical predictions and the experimental results in all cases, although for NR

samples, having a strength at least 10 times larger than for SBR, the results from T-peel were significantly higher than from 90° peel, as noted before for T-peel from perforated plates. This anomaly is attributed to the same effect: when only one or two rows of strands carry the entire peel force, the integration upon which Equations 11 and 12 are based is no longer appropriate.

5 Conclusions

When an elastic adhesive layer penetrates into pores in a rigid substrate, extra work is expended in debonding the layer because the material in the pores is stretched as it is pulled out. The extra work can be estimated for a simple linearly-elastic adhesive, using a fracture energy criterion for debonding. The theory predicts that the extra work is proportional to the fractional area of surface occupied by pores, and to the ratio of depth to diameter of the pores.

Experiments with a layer of natural rubber vulcanized in contact with model porous surfaces gave good agreement with the theoretical predictions, the apparent work of detachment being increased by a factor of up to 20X. (It should be noted that the apparent work of detachment can exceed the work of rupture of the adhesive layer itself, without any of the material actually breaking.)

When the pores are deep or interconnected, however, the strands of adhesive within them will break rather than pull out. The extra work from this process has been evaluated for some simple cases. It was as much as several hundred times the (low) work of detachment from a

smooth substrate, in good agreement with theoretical predictions that take into account the work of strand rupture. In this case, the additional work is proportional to the depth of the pores, and thus it will become the dominant term for deep pores.

Measurements were also made of the work of separating a vulcanized rubber layer from a sheet of open-weave wire cloth that the rubber had permeated. Again, the work of detachment was greatly increased by the extra work of breaking strands of rubber, in reasonable agreement with the theory incorporating the work of strand rupture.

Acknowledgements

This work forms part of a program of research on adhesion supported by the Office of Naval Research (Contract No. N00014-85-K-0222, Project Officer: Dr.R.S.Miller) and by grants-in-aid from 3M Company, Westvaco, and Lord Corporation.

References

1. H.Narcus, Trans. Plast. Inst. 35, 529 (1967).
2. C.W.Jennings, J.Adhesion 4, 25 (1972).
3. D.E.Packham, K.Bright and B.W.Malpass, J.Appl.Polym.Sci. 18, 3237, 3249 (1974).
4. A.J.Kinloch, "Adhesion and Adhesives: Science and Technology", Chapman and Hall, London, 1987.
5. W.C.Wake, "Adhesion and the Formulation of Adhesives", Appl. Sci. Publishers, Ltd. London, 1982, Chap. 15.
6. A.N.Gent, G.S.Fielding-Russell, D.I.Livingston and D.W.Nicholson, J.Mater.Sci. 17, 1713 (1982).
7. A.N.Gent and A.G.Thomas, Rubber Chem.Technol. 36, 597 (1963).

Appendix

Mix recipes and vulcanization conditions employed to prepare the rubber layers were as follows:

Elastomer, 100; zinc oxide, 5; stearic acid, 2; accelerator (Santocure), 1; sulfur, 2.5 (NR) or 2 (SBR). Vulcanization was effected by heating for 30 min at 141° C for NR and 60 min at 145° C for SBR.

The elastomers used were natural rubber (pale crepe) and a styrene-butadiene copolymer containing 23.5% styrene and 76.5% butadiene (Plioflex 1502, The Goodyear Tire and Rubber Company).

Table 1. Characterization of square-woven stainless steel cloth

Sample	Wire diam. \underline{d} ($= \underline{\ell}/2$, mm)	Length \underline{s} of side of holes (mm)	Number of holes \underline{n} ($\times 10^{-6}$, m^{-2})	φ ($= \underline{n}\underline{s}^2$)
1	0.585	1.02	0.38	0.39
2	0.585	0.685	0.62	0.29
3	0.33	0.51	1.44	0.375
4	0.28	0.152	5.05	0.115
5	0.19	0.127	9.95	0.16
6	0.305	0.585	1.45	0.50

Table 2. Work G'_a of peeling NR layers from Al plates, perforated
with holes of depth l and radius a

l (mm)	a (mm)	l/a	φ	G'_a (calc. from Eq. 7) (J/m^2)	G'_a (meas.) (J/m^2)
1.62	0.77	2.12	0.10	65	105 ± 35
1.62	0.77	2.12	0.23	103	105 ± 35
1.62	0.77	2.12	0.37	145	195 ± 35
2.3	1.25	1.85	0.42	144	155 ± 20
2.3	1.25	1.85	0.53	172	185 ± 25
2.3	0.77	3.00	0.10	77	130 ± 35
2.3	0.77	3.00	0.16	102	65 ± 20
2.3	0.77	3.00	0.23	132	110 ± 20
3.12	0.77	4.05	0.10	92	135 ± 35
3.12	0.77	4.05	0.15	120	190 ± 35
3.12	0.77	4.05	0.23	165	195 ± 25
3.12	0.77	4.05	0.33	222	255 ± 45
6.55	0.82	8.0	0.40	482	540 ± 50
6.55	0.82	8.0	0.53	629	685 ± 40
6.55	1.00	6.55	0.43	429	505 ± 40
6.55	1.15	5.65	0.41	360	410 ± 40
9.2	0.82	11.2	0.40	663	735 ± 110
9.2	1.30	7.05	0.42	450	410 ± 80

Table 3. Tearing NR and SBR layers away from perforated Al plates

(a) <u>NR Layers</u>			
$n \times 10^{-4}$ (m^{-2})	G'_a (90° peel) (kJ/m^2)	G'_a (T - peel) (kJ/m^2)	G'_a (calc. from Eq.13) (kJ/m^2)
[$l = 1.62$ mm, $a = 0.76$ mm]			
5.45	3.9 ± 1	5.65 ± 2	3.05
8.65	5.25 ± 1	8.3 ± 1	4.85
12.5	7.6 ± 1.5	11.3 ± 1.3	7.05
20	10.8 ± 1	16.5 ± 1	11.3
[$l = 2.3$ mm, $a = 0.76$ mm]			
5.45	4.9 ± 0.75	6.6 ± 1.5	4.35
8.65	7.6 ± 1	10.1 ± 2	6.92
12.5	10.3 ± 1.5	13.7 ± 2	10.0
[$l = 3.12$ mm, $a = 0.79$ mm]			
5.45	6.05 ± 1	10.8 ± 2.5	6.05
8.35	8.6 ± 0.8	13.5 ± 2.5	9.3
12.5	13.2 ± 1.5	19.5 ± 2.5	13.9
[$l = 1.58$ mm, $a = 0.50$ mm]			
8.75	2.45 ± 0.4	4.4 ± 0.7	2.05
12.5	3.1 ± 0.4	3.9 ± 0.8	2.95
25	6.1 ± 0.8	10.8 ± 1	5.90

Table 3 (cont.)

(b) <u>SBR Layers</u>			
$\bar{n} \times 10^{-4}$ (m^{-2})	\underline{G}_a' (90° peel) (kJ/m^2)	\underline{G}_a' (T - peel) (kJ/m^2)	\underline{G}_a' (calc. from Eq.13) (kJ/m^2)
[$\ell = 1.62$ mm, $a = 0.76$ mm]			
5.45	0.72 ± 0.15	0.88 ± 0.2	0.49
8.65	1.1 ± 0.15	1.4 ± 0.3	0.78
12.5	1.8 ± 0.12	1.75 ± 0.35	1.13
20	2.5 ± 0.1	2.7 ± 0.5	1.80
[$\ell = 2.30$ mm, $a = 0.76$ mm]			
5.45	0.98 ± 0.25	1.18 ± 0.3	0.70
8.65	1.25 ± 0.25	1.45 ± 0.25	1.10
12.5	2.20 ± 0.05	2.25 ± 0.3	1.60
[$\ell = 3.12$ mm, $a = 0.79$ mm]			
5.45	1.20 ± 0.4	1.75 ± 0.5	1.00
8.35	1.6 ± 0.1	2.2 ± 0.5	1.55
12.5	2.5 ± 0.15	3.4 ± 0.5	2.35
[$\ell = 1.58$ mm, $a = 0.50$ mm]			
8.75	0.51 ± 0.03	0.66 ± 0.15	0.33
12.5	0.64 ± 0.03	0.66 ± 0.05	0.47
25	1.20 ± 0.12	1.30 ± 0.15	0.95

Figure Legends

Figure 1. (a) Sketch of rubber layer peeling from a perforated plate at 90° .

(b) T-peel separation of two rubber layers connected by strands passing through a perforated plate.

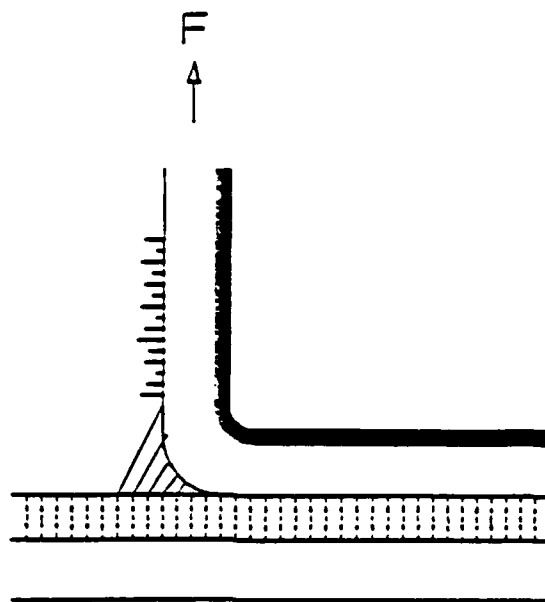
Figure 2. Effective work \underline{G}_a' of detachment for layers of NR vulcanized in contact with perforated Al plates, plotted against the porosity parameter $\varphi(\underline{l}/\underline{a})$ in accordance with Equation 7, for holes of various depths \underline{l} in the range 1.6 to 9 mm, radii \underline{a} in the range 0.8 to 1.3 mm, and occupying a fraction φ of the plate area ranging from 0.1 to 0.5. The full line represents the predictions of Equation 7.

Figure 3. Effective work \underline{G}_a' of detachment for layers of NR vulcanized in contact with the two sides of a perforated Al plate and joined together by interconnecting strands, plotted against the porosity parameter $\varphi \underline{l}$ in accordance with Equation 13. The full line represents the predictions of Equation 13.

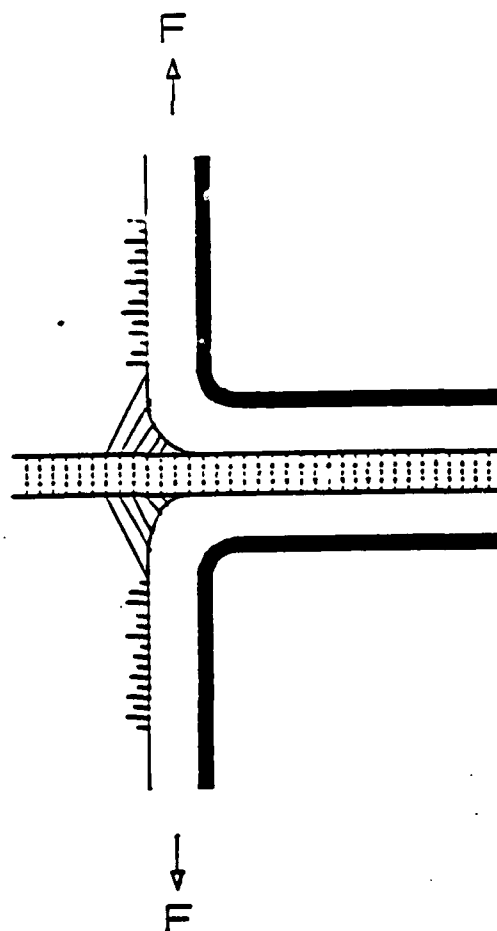
Figure 4. Effective work \underline{G}_a' of detachment for layers of SBR vulcanized in contact with the two sides of a perforated Al plate and joined together by interconnecting strands, plotted against the porosity parameter $\varphi \underline{l}$ in accordance with Equation 13. The full line represents the predictions of Equation 13.

Figure 5. Effective work \underline{G}_a' of detachment for a layer of NR vulcanized in contact with a sheet of open-weave stainless steel wire cloth and joined to a similar layer on the other side by interconnecting strands, plotted against the porosity parameter ϕ_l in accordance with Equation 13. The full line represents the predictions of Equation 13.

Figure 6. Effective work \underline{G}_a' of detachment for a layer of SBR vulcanized in contact with a sheet of open-weave stainless steel wire cloth and joined to a similar layer on the other side by interconnecting strands, plotted against the porosity parameter ϕ_l in accordance with Equation 13. The full line represents the predictions of Equation 13.



(a)



(b)

FIGURE 1

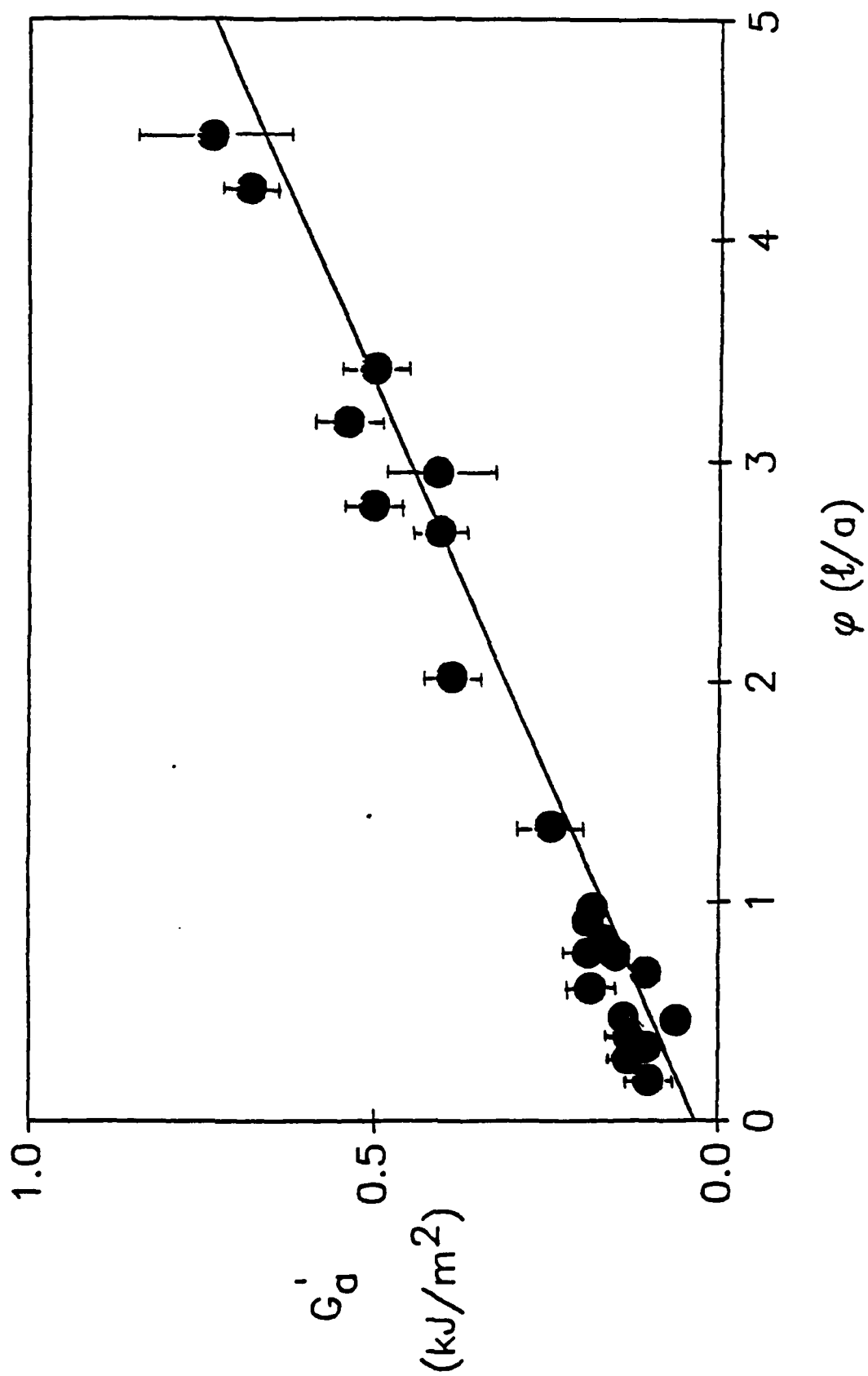


FIGURE 2

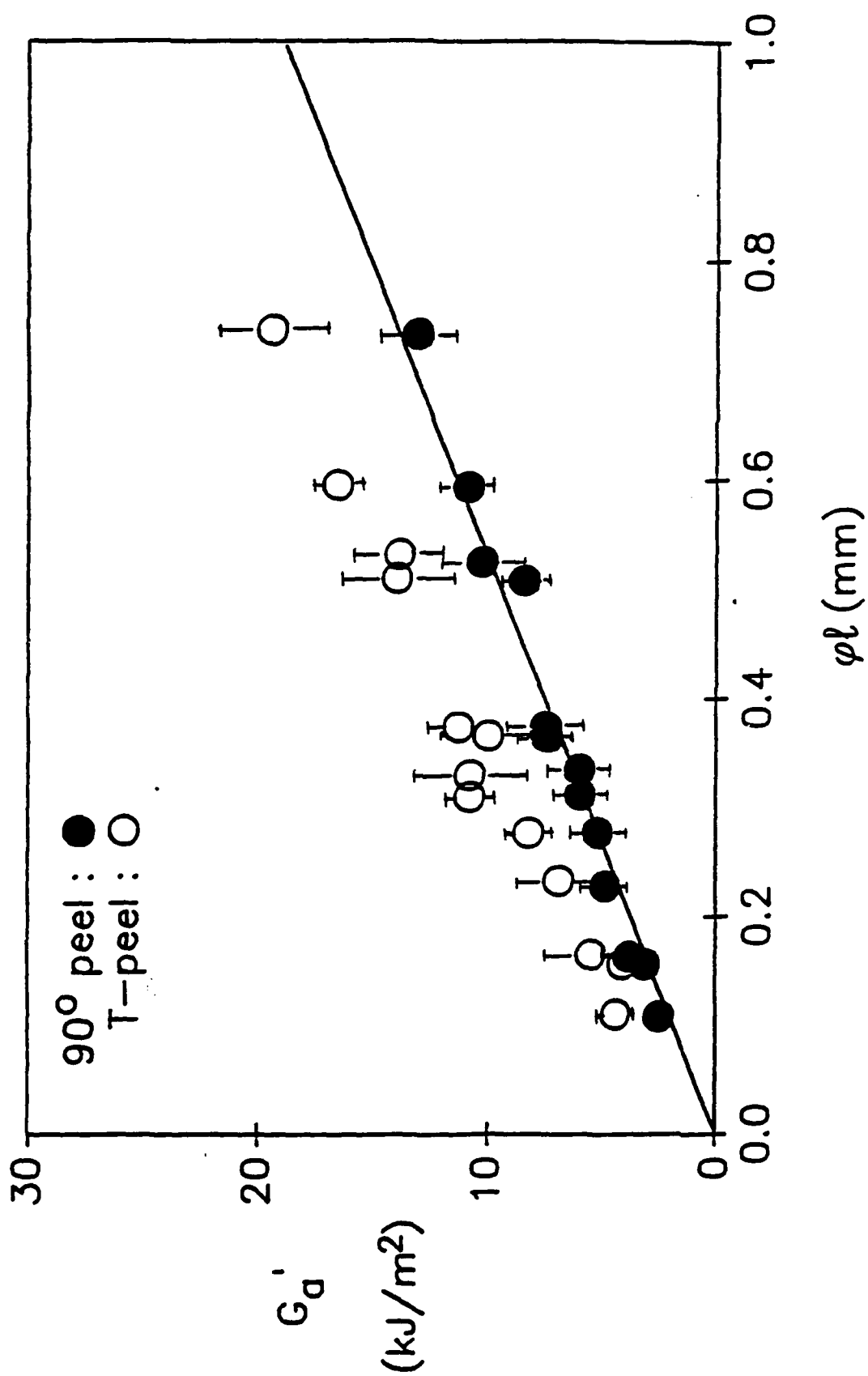


FIGURE 3

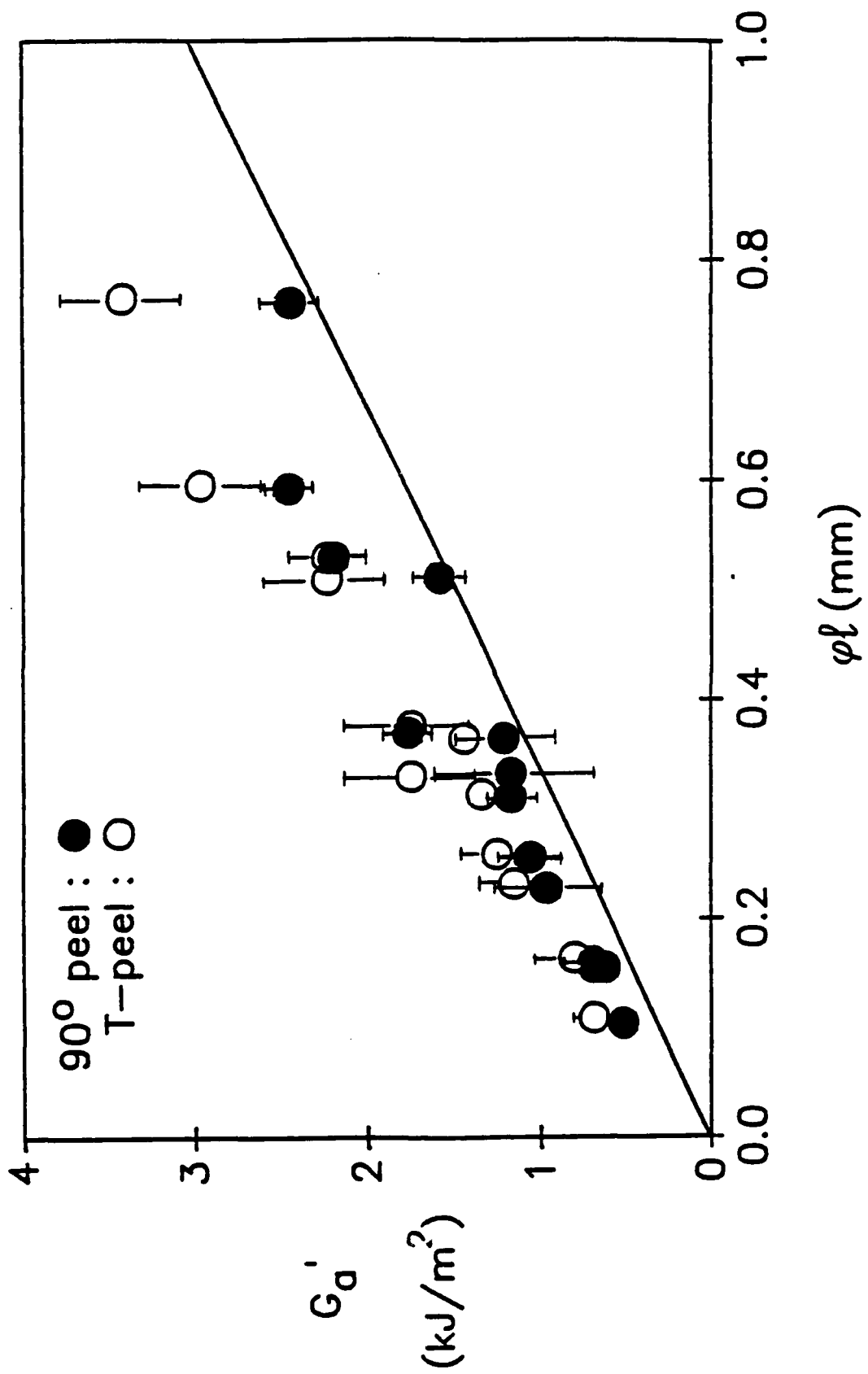


FIGURE 4

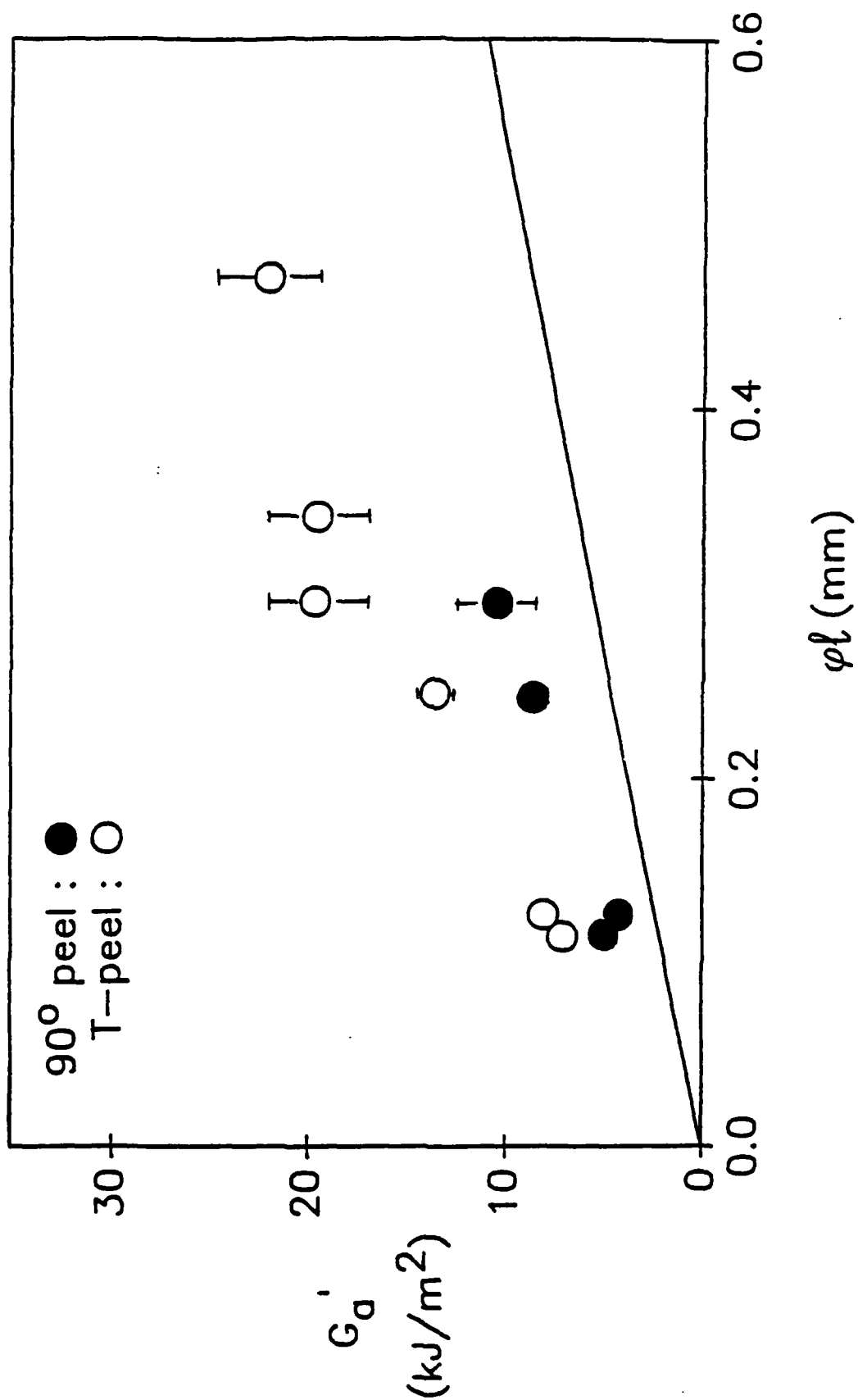


FIGURE 5

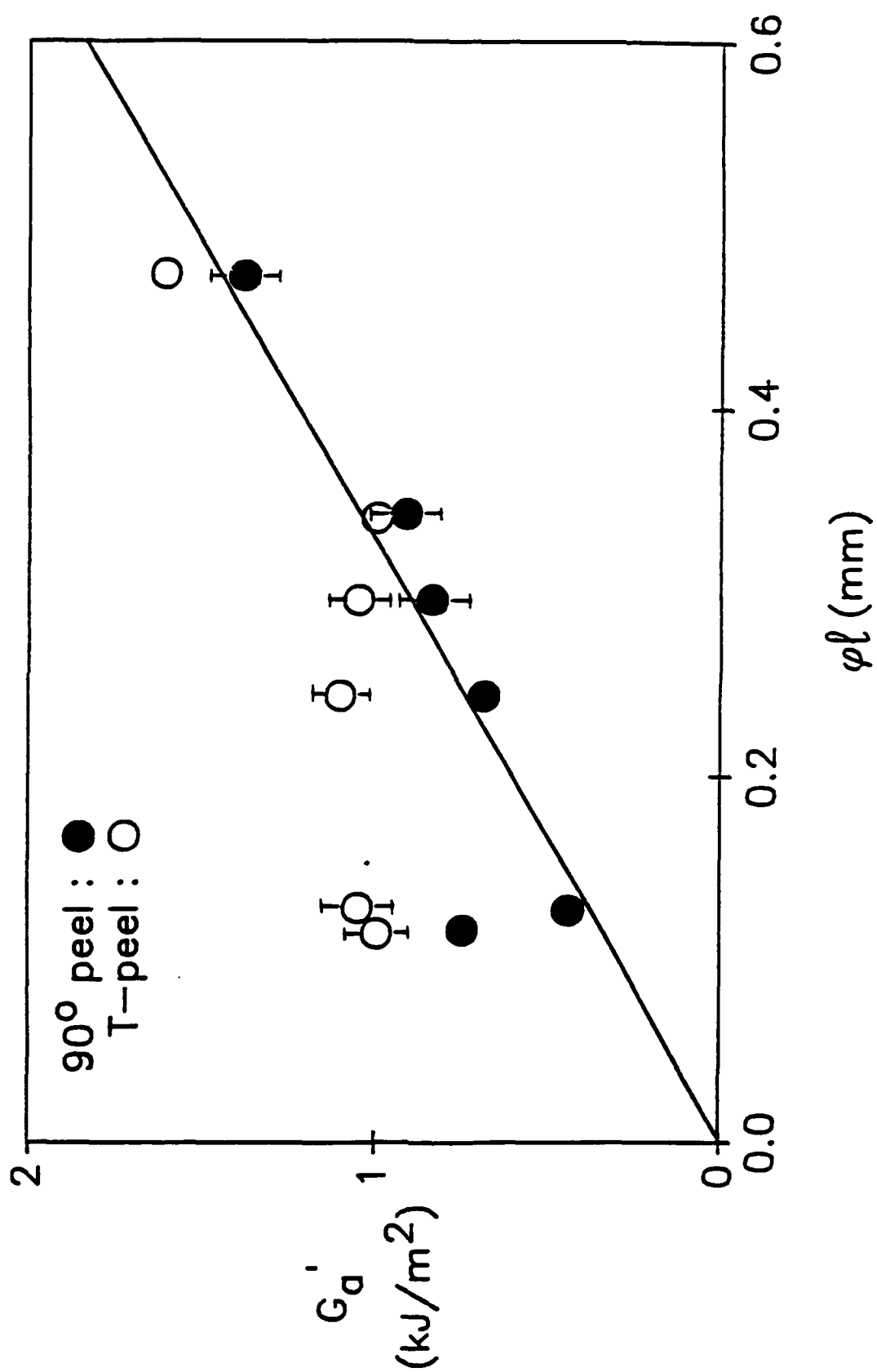


FIGURE 6

(DYN)

DISTRIBUTION LIST

Mr. R. Geisler
ATTN: DY/MS-24
AFRPL
Edwards AFB, CA 93523

Naval Air Systems Command
ATTN: Mr. Bertram P. Sobers
NAVAIR-320G
Jefferson Plaza 1, RM 472
Washington, DC 20361

R.B. Steele
Aerojet Strategic Propulsion Co.
P.O. Box 15699C
Sacramento, CA 95813

Mr. M. Stosz
Naval Surface Weapons Center
Code R10B
White Oak
Silver Spring, MD 20910

Mr. S.F. Palopali
Thiokol Corporation
Elkton Division
P.O. Box 241
Elkton, MD 21921

Dr. Grant Thompson
Morton Thiokol, Inc.
Wasatch Division
MS 240 P.O. Box 524
Brigham City, UT 84302

Dr. R.S. Valentini
United Technologies Chemical Systems
P.O. Box 50015
San Jose, CA 95150-0015

Dr. R.F. Walker
Chief, Energetic Materials Division
DRSMC-LCE (D), B-3022
USA ARDC
Dover, NJ 07801

~~Dr. Janet Wall
Code 012
Director, Research Administration
Naval Postgraduate School
Monterey, CA 93943~~

Director
US Army Ballistic Research Lab.
ATTN: DRXBR-IBD
Aberdeen Proving Ground, MD 21005

Commander
US Army Missile Command
ATTN: DRSMI-RKL
Walter W. Wharton
Redstone Arsenal, AL 35898

Dr. Ingo W. May
Army Ballistic Research Lab.
ARRADCOM
Code DRXBR - 1BD
Aberdeen Proving Ground, MD 21005

Dr. E. Zimet
Office of Naval Technology
Code 071
Arlington, VA 22217

Dr. Ronald L. Derr
Naval Weapons Center
Code 389
China Lake, CA 93555

~~T. Boggs
Naval Weapons Center
Code 389
China Lake, CA 93555~~

Lee C. Estabrook, P.E.
Morton Thiokol, Inc.
P.O. Box 30058
Shreveport, Louisiana 71130

Dr. J.R. West
Morton Thiokol, Inc.
P.O. Box 30058
Shreveport, Louisiana 71130

Dr. D.D. Dillehay
Morton Thiokol, Inc.
Longhorn Division
Marshall, TX 75670

G.T. Bowman
Atlantic Research Corp.
7511 Wellington Road
Gainesville, VA 22065

(DYN)

DISTRIBUTION LIST

Dr. R.S. Miller
Office of Naval Research
Code 432P
Arlington, VA 22217
(10 copies)

Dr. J. Pastine
Naval Sea Systems Command
Code 06R
Washington, DC 20362

~~Dr. Kenneth D. Hartman
Hercules Aerospace Division
Hercules Incorporated
Allegheny Ballistic Lab
P.O. Box 210
Cumberland, MD 20502~~

~~Mr. Otto K. Heiney
AFATL-DL-16
Elgin AFB, FL 32542~~

Dr. Merrill K. King
Atlantic Research Corp.
5390 Cherokee Avenue
Alexandria, VA 22312

Dr. R.L. Lou
Aerojet Strategic Propulsion Co.
Bldg. 05025 - Dept 5400 - MS 167
P.O. Box 15699C
Sacramento, CA 95813

Dr. R. Olsen
Aerojet Strategic Propulsion Co.
Bldg. 05025 - Dept 5400 - MS 167
P.O. Box 15699C
Sacramento, CA 95813

Dr. Randy Peters
Aerojet Strategic Propulsion Co.
Bldg. 05025 - Dept 5400 - MS 167
P.O. Box 15699C
Sacramento, CA 95813

Dr. D. Mann
U.S. Army Research Office
Engineering Division
Box 12211
Research Triangle Park, NC 27709-2211

Dr. L.V. Schmidt
Office of Naval Technology
Code 07CT
Arlington, VA 22217

JHU Applied Physics Laboratory
ATTN: CPIA (Mr. T.W. Christian)
Johns Hopkins Rd.
Laurel, MD 20707

Dr. R. McGuire
Lawrence Livermore Laboratory
University of California
Code L-324
Livermore, CA 94550

P.A. Miller
736 Leavenworth Street, #6
San Francisco, CA 94109

Dr. W. Moniz
Naval Research Lab.
Code 6120
Washington, DC 20375

Dr. K.F. Mueller
Naval Surface Weapons Center
Code R11
White Oak
Silver Spring, MD 20910

Prof. M. Nicol
Dept. of Chemistry & Biochemistry
University of California
Los Angeles, CA 90024

Mr. L. Roslund
Naval Surface Weapons Center
Code R10C
White Oak, Silver Spring, MD 20910

Dr. David C. Sayles
Ballistic Missile Defense
Advanced Technology Center
P.O. Box 1500
Huntsville, AL 35807

(DYN)

DISTRIBUTION LIST

R.E. Shenton
Atlantic Research Corp.
7511 Wellington Road
Gainesville, VA 22065

Mike Barnes
Atlantic Research Corp.
7511 Wellington Road
Gainesville, VA 22065

Dr. Lionel Dickinson
Naval Explosive Ordnance
Disposal Tech. Center
Code D
Indian Head, MD 20340

Prof. J.T. Dickinson
Washington State University
Dept. of Physics 4
Pullman, WA 99164-2814

M.H. Miles
Dept. of Physics
Washington State University
Pullman, WA 99164-2814

Dr. T.F. Davidson
Vice President, Technical
Morton Thiokol, Inc.
Aerospace Group
3340 Airport Rd.
Ogden, UT 84405

Mr. J. Consaga
Naval Surface Weapons Center
Code R-16
Indian Head, MD 20640

Naval Sea Systems Command
ATTN: Mr. Charles M. Christensen
NAVSEA-62R2
Crystal Plaza, Bldg. 6, Rm 806
Washington, DC 20362

Mr. R. Beauregard
Naval Sea Systems Command
SEA 64E
Washington, DC 20362

Brian Wheatley
Atlantic Research Corp.
7511 Wellington Road
Gainesville, VA 22065

Mr. G. Edwards
Naval Sea Systems Command
Code 62R32
Washington, DC 20362

C. Dickinson
Naval Surface Weapons Center
White Oak, Code R-13
Silver Spring, MD 20910

Prof. John Deutch
MIT
Department of Chemistry
Cambridge, MA 02139

~~Dr. E.H. deButts
Hercules Aerospace Co.
P.O. Box 27408
Salt Lake City, UT 84127~~

David A. Flanigan
Director, Advanced Technology
Morton Thiokol, Inc.
Aerospace Group
~~2475 Washington Blvd.~~
Ogden, UT 84401

Dr. L.H. Caveny
Air Force Office of Scientific
Research
Directorate of Aerospace Sciences
Bolling Air Force Base
Washington, DC 20332

~~W.G. Roger
Code 5253
Naval Ordnance Station
Indian Head, MD 20640~~

Dr. Donald L. Ball
Air Force Office of Scientific
Research
Directorate of Chemical &
Atmospheric Sciences
Bolling Air Force Base
Washington, DC 20332

(DYN)

DISTRIBUTION LIST

Dr. Anthony J. Matuszko
Air Force Office of Scientific Research
Directorate of Chemical & Atmospheric
Sciences
Bolling Air Force Base
Washington, DC 20332

Dr. Michael Chaykovsky
Naval Surface Weapons Center
Code R11
White Oak
Silver Spring, MD 20910

J.J. Rocchio
USA Ballistic Research Lab.
Aberdeen Proving Ground, MD 21005-5066

B. Swanson
INC-4 MS C-346
Los Alamos National Laboratory
Los Alamos, New Mexico 87545

Dr. James T. Bryant
Naval Weapons Center
Code 3205B
China Lake, CA 93555

Dr. L. Rothstein
Assistant Director
Naval Explosives Dev. Engineering Dept.
Naval Weapons Station
Yorktown, VA 23691

~~Dr. M.J. Kamlet
Naval Surface Weapons Center
Code R11
White Oak, Silver Spring, MD 20910~~

Dr. Henry Webster, III
Manager, Chemical Sciences Branch
ATTN: Code 5063
Crane, IN 47522

Dr. A.L. Slafkosky
Scientific Advisor
Commandant of the Marine Corps
Code RD-1
Washington, DC 20380

Dr. H.G. Adolph
Naval Surface Weapons Center
Code R11
White Oak
Silver Spring, MD 20910

U.S. Army Research Office
Chemical & Biological Sciences
Division
P.O. Box 12211
Research Triangle Park, NC 27709

Dr. John S. Wilkes, Jr.
FJSRL/NC
USAF Academy, CO 80840

Dr. H. Rosenwasser
AIR-320R
Naval Air Systems Command
Washington, DC 20361

Dr. Joyce J. Kaufman
The Johns Hopkins University
Department of Chemistry
Baltimore, MD 21218

Dr. A. Nielsen
Naval Weapons Center
Code 385
China Lake, CA 93555

(DYN)

DISTRIBUTION LIST

K.D. Pae
High Pressure Materials Research Lab.
Rutgers University
P.O. Box 909
Piscataway, NJ 08854

Prof. Edward Price
Georgia Institute of Tech.
School of Aerospace Engineering
Atlanta, GA 30332

Dr. John K. Dienes
T-3, B216
Los Alamos National Lab.
P.O. Box 1663
Los Alamos, NM 87544

~~S.A. Birkett
Naval Ordnance Station
Code 5253K
Indian Head, MD 20640~~

A.N. Gent
Institute Polymer Science
University of Akron
Akron, OH 44325

Prof. R.W. Armstrong
University of Maryland
Dept. of Mechanical Engineering
College Park, MD 20742

Dr. D.A. Shockey
SRI International
333 Ravenswood Ave.
Menlo Park, CA 94025

Herb Richter
Code 385
Naval Weapons Center
China Lake, CA 93555

Dr. R.B. Kruse
Morton Thiokol, Inc.
Huntsville Division
Huntsville, AL 35807-7501

~~J.T. Rosenberg
SRI International
333 Ravenswood Ave.
Menlo Park, CA 94025~~

G. Butcher
Hercules, Inc.
P.O. Box 98
Magna, UT 84044

G.A. Zimmerman
Aerojet Tactical Systems
P.O. Box 13400
Sacramento, CA 95813

W. Waesche
Atlantic Research Corp.
7511 Wellington Road
Gainesville, VA 22065

Prof. Kenneth Kuo
Pennsylvania State University
Dept. of Mechanical Engineering
University Park, PA 16802

Dr. R. Bernecker
Naval Surface Weapons Center
Code R13
White Oak
Silver Spring, MD 20910

T.L. Boggs
Naval Weapons Center
Code 3891
China Lake, CA 93555

(DYN)

DISTRIBUTION LIST

Dr. C.S. Coffey
Naval Surface Weapons Center
Code R13
White Oak
Silver Spring, MD 20910

D. Curran
SRI International
333 Ravenswood Avenue
Menlo Park, CA 94025

E.L. Throckmorton
Code SP-2731
Strategic Systems Program Office
Crystal Mall #3, RM 1048
Washington, DC 23076

R.G. Rosemeier
Brimrose Corporation
7720 Belair Road
Baltimore, MD 20742

C. Gotzmer
Naval Surface Weapons Center
Code R-11
White Oak
Silver Spring, MD 20910

G.A. Lo
3251 Hanover Street
B204 Lockheed Palo Alto Research Lab
Palo Alto, CA 94304

R.A. Schapery
Civil Engineering Department
Texas A&M University
College Station, TX 77843

Dr. Y. Gupta
Washington State University
Department of Physics
Pullman, WA 99163

J.M. Culver
Strategic Systems Projects Office
SSPO/SP-2731
Crystal Mall #3, RM 1048
Washington, DC 20376

Prof. G.D. Duvall
Washington State University
Department of Physics
Pullman, WA 99163

Dr. E. Martin
Naval Weapons Center
Code 3858
China Lake, CA 93555

Dr. M. Farber
135 W. Maple Avenue
Monrovia, CA 91016

W.L. Elban
Naval Surface Weapons Center
White Oak, Bldg. 343
Silver Spring, MD 20910

Defense Technical Information Center
Bldg. 5, Cameron Station
Alexandria, VA 22314
(12 copies)

Dr. Robert Polvani
National Bureau of Standards
Metallurgy Division
Washington, D.C. 20234

Director
Naval Research Laboratory
Attn: Code 2627
Washington, DC 20375
(6 copies)

Administrative Contracting
Officer (see contract for
address)
(1 copy)